Soliton fission and supercontinuum generation in silicon waveguides

Lianghong Yin, Qiang Lin, and Govind P. Agrawal

Institute of Optics, University of Rochester, Rochester, New York, 14627, USA

Received August 31, 2006; revised October 31, 2006; accepted November 2, 2006;
posted November 14, 2006 (Doc. ID 74663); published January 26, 2007

We show through numerical simulations that silicon waveguides can be used to create a supercontinuum extending over 400 nm by launching femtosecond pulses as higher-order solitons. The physical process behind continuum generation is related to soliton fission, self-phase modulation, and generation of Cherenkov radiation. In contrast with optical fibers, stimulated Raman scattering plays little role. As low-energy ($\approx$1 pJ) pulses and short waveguides ($<$1 cm) are sufficient for continuum generation, the proposed scheme should prove useful for practical applications. © 2007 Optical Society of America

OCIS codes: 190.4360, 190.5530, 190.7110, 160.4330.

Many applications such as optical coherence tomography and high-precision metrology require an ultrabroadband light source. Highly nonlinear fibers in combination with a mode-locked laser can be used to provide such a source through the process called supercontinuum generation.[1,2] In recent years, silicon-on-insulator (SOI) waveguides have been used for several nonlinear effects such as Raman amplification, four-wave mixing, and self-phase modulation.[3–10] It has been realized that such waveguides can support solitons in the wavelength region near 1.5 μm, if they are designed suitably to provide anomalous dispersion.[11] Although nonlinear spectral broadening has been observed earlier,[5,6] the bandwidth was limited to $\sim$10 nm or so. In this paper, we show theoretically that the fission of higher-order solitons inside SOI waveguides can generate a supercontinuum that is more than 400 nm wide. To be realistic, we include in our analysis both the two-photon absorption (TPA) and the free-carrier absorption (FCA), in addition to stimulated Raman scattering (SRS), and show that TPA is not detrimental to the supercontinuum process, even though it reduces the spectral broadening to some extent.

Silicon waveguides and silica fibers differ in many respects, the most important being that the length of a silicon waveguide rarely exceeds 5 cm in practice, whereas silica fibers can be many meters long. Fortunately, silicon exhibits a Kerr nonlinearity more than 200 times larger than that of silica. Moreover, its relatively large refractive index allows silicon waveguides to confine light within an area so small that nonlinear effects can be enhanced by more than a factor of 10,000. Another major difference is related to the crystalline nature of silicon that makes SRS depend strongly on the waveguide geometry and mode polarization.[8] In particular, for an SOI waveguide fabricated along the $[\bar{1}10]$ direction on the (001) surface, SRS cannot occur when an input pulse excites the TM mode. To include the impact of SRS, we focus on the TE mode in this study.

Soliton formation requires that the SOI waveguide exhibit anomalous dispersion at the operating wavelength near 1.55 μm. We have shown that the zero-dispersion wavelength (ZDWL) of such waveguides can be tailored to fall in this regime with a suitable design.[11] We have also found that the ZDWL of both the TE and TM modes can be below 1.55 μm for a ridge waveguide geometry shown as the inset in Fig. 1 when both the width and height of the waveguide are close to 0.8 μm.[8] We focus on such a waveguide and assume that $W=0.8$ μm and $H=0.7$ μm.

The supercontinuum process employs ultrashort pulses and depends strongly on the material dispersion. For this reason, we need to know the refractive index n_{Si} of silicon accurately over the wavelength range of interest (1.2 to 2.0 μm). We use the data from Ref. 12 with curve fitting and model n_{Si} accurately with the following Sellmeier-type relation:

$$n_{\mathrm{Si}}^2(\nu) = 1 + \frac{c_1}{1-(h\nu/E_1)^2} + \frac{c_2}{1-(h\nu/E_2)^2}, \qquad (1)$$

where $h\nu$ is the photon energy, $E_1=4.27$ eV, $E_2=3.38$ eV, $c_1=9.733$, and $c_2=0.936$. We calculate the effective mode index n_{eff} and its wavelength dependence with a full-vector finite difference mode solver.[13] The ZDWL of the fundamental TE mode is found to be 1496 nm. The effective mode area is $a_{\mathrm{eff}}=0.32$ μm^2 at $\lambda_0=1550$ nm. The wavelength dependences of n_{Si}, n_{eff}, and second-order dispersion β_2 are shown in Fig. 1. Although such a waveguide supports multiple modes, our analysis shows that the phase velocities and mode profiles differ substantially for the fundamental mode and high-order modes. As a result, intermodal coupling is not likely to participate in the soliton fission process. Although we focus on a specific waveguide geometry, our results should apply to any waveguide designed to produce dispersion parameters close to those used here.

To study supercontinuum generation, we launch a femtosecond pulse polarized such that it excites the fundamental TE mode and propagates in the form of a high-order soliton. Its evolution is governed by the same generalized nonlinear Schrödinger equation

0146-9592/07/040391-3/$15.00

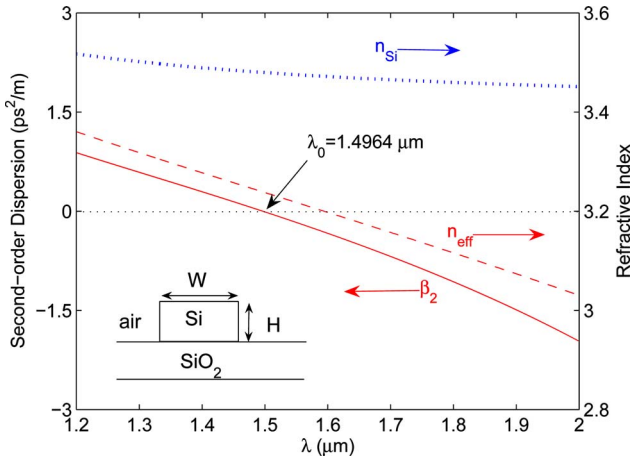

Fig. 1. (Color online) Wavelength dependence of n_{Si} (dotted curve), n_{eff} (dashed curve), and β_2 (solid curve) for the fundamental TE mode using the waveguide shown in the inset with $W=0.8$ μm and $H=0.7$ μm.

used for fibers[2] but modified as folows to include the effects of TPA and FCA[11]:

$$\frac{\partial A}{\partial z}=i\sum_{m=2}^{\infty}\frac{i^m\beta_m}{m!}\frac{\partial^m A}{\partial t^m}+i\gamma\left(1+\frac{i}{\omega_0}\frac{\partial}{\partial t}\right)A(z,t)\times\int_{-\infty}^{t}R(t-t')|A(z,t')|^2\mathrm{d}t'-\frac{1}{2}(\alpha_l+\alpha_f)A, \quad (2)$$

where α_l and α_f account for linear losses and FCA, respectively. The nonlinear parameter γ is complex because of the TPA effects and is defined as

$$\gamma=\frac{2\pi n_2}{\lambda a_{\mathrm{eff}}}+i\frac{\beta_{\mathrm{TPA}}}{2a_{\mathrm{eff}}}, \quad (3)$$

where $\beta_{\mathrm{TPA}}=5\times10^{-12}$ m/W is the TPA parameter.[8]

The magnitude of FCA is obtained from $\alpha_f=\sigma N_c(z,t)$, where N_c is the density of free carriers and $\sigma=1.45\times10^{-21}$ m^2 for silicon.[8] The density N_c produced by TPA is obtained by solving

$$\frac{\partial N_c(z,t)}{\partial t}=\frac{\beta_{\mathrm{TPA}}}{2h\nu_0}\frac{|A(z,t)|^4}{a_{\mathrm{eff}}^2}-\frac{N_c(z,t)}{\tau}, \quad (4)$$

where τ is the effective carrier lifetime, estimated to be about 3 ns.[4] For femtosecond pulses used here and at relatively low repetition rates, $N_c\leqslant 2\beta_{\mathrm{TPA}}P_0^2T_0/(3h\nu_0a_{\mathrm{eff}}^2)$, where P_0 is the peak power of a "sech" pulse of width $T_p\approx1.76T_0$. The wavelength dependence of γ and σ is neglected in this study; it can be included following a standard approach.[2,4]

A soliton of order N is excited if $A(0,t)=\sqrt{P_0}\,\mathrm{sech}(t/T_0)$ initially, and the input parameters satisfy the condition $N^2=\mathrm{Re}(\gamma)P_0T_0^2/|\beta_2|$. We solve Eq. (2) with the split-step Fourier method[2] for a third-order soliton ($N=3$) using $T_p=50$ fs. The peak power P_0 equals 25 W using $n_2=6\times10^{-18}$ m^2/W and $\beta_2=-0.1701$ ps^2/m (estimated from Fig. 1 at $\lambda_0=1.55$ μm). We estimate a maximum carrier density of $N_c\approx8\times10^{21}$ m^{-3}, resulting in $\alpha_f\approx11.6$ m^{-1} after all carriers have been generated. The corresponding carrier-induced index change,[14] $\Delta n_c\approx-1\times10^{-5}$, is too small to affect soliton propagation. Numerically, we solve the coupled set of Eqs. (2) and (4) to include all time-dependent features of TPA and FCA.

Before proceeding, we need to specify the nonlinear response function $R(t)$ appearing in Eq. (2). Similar to the case of silica fibers, we use the form $R(t)=(1-f_R)\delta(t)+f_Rh_R(t)$, where the first term governs the nearly instantaneous electronic response and $h_R(t)$ is the Raman response function.[2] The parameter f_R represents the fractional contribution of the nuclei to the total nonlinear polarization. The functional form of the Raman response function $h_R(t)$ is deduced from the Raman gain spectrum, $g_R(\Omega)$, known to exhibit a narrow Lorentzian peak of $\approx$105 GHz bandwidth, located 15.6 THz away from the pump frequency.[15] The imaginary part of the Fourier transform $H_R(\Omega)$ of $h_R(t)$ is related to $g_R(\Omega)$ as $\mathrm{Im}[H_R(\Omega)]=g_R(\Omega)/(2k_0n_2f_R)$, where $k_0=2\pi/\lambda_0$. We use the value $g_R^{\max}=2\times10^{-10}$ m/W at the Raman gain peak.[8] The real part of $H_R(\Omega)$ is then found from the Kramers–Kronig relation. Once $H_R(\Omega)$ is known, $h_R(t)$ is obtained by taking its inverse Fourier transform. The parameter f_R is found to be 0.043 from the normalization condition of $\int_0^\infty h_R(t)\mathrm{d}t=1$; this value is relatively small compared with $f_R=0.18$ for silica fibers.[2]

As seen in Eq. (2), soliton evolution is affected by dispersion to all orders ($m>1$). Often, the sum is truncated to include the dispersion terms up to $m=6$ or 7.[2] A better approach is to notice that the infinite series can be written in the frequency domain as

$$\mathcal{F}\left[\sum_{m=2}^{\infty}i\frac{i^m\beta_m}{m!}\frac{\partial^m A}{\partial t^m}\right]=[\beta(\omega)-\beta(\omega_0)-\beta_1(\omega_0)(\omega-\omega_0)]\tilde{A}(\omega), \quad (5)$$

where $\beta(\omega)=n_{\mathrm{eff}}(\omega)\omega/c$, $\beta_1(\omega)=\partial\beta/\partial\omega$, and $\mathcal{F}$ is the Fourier transform operator. We include dispersion to all orders by using Eq. (5) with $n_{\mathrm{eff}}(\omega)$ from Fig. 1.

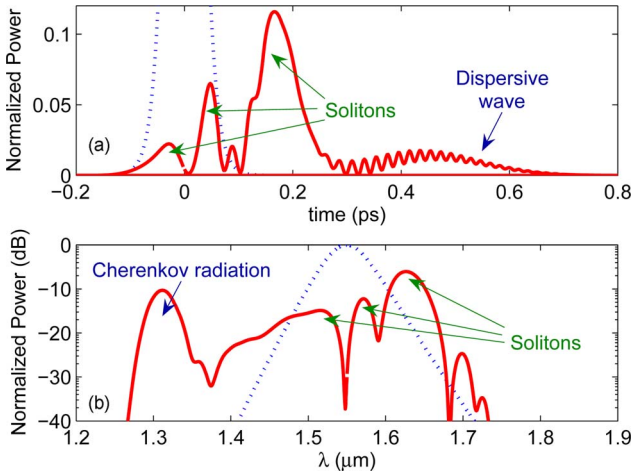

Fig. 2. (Color online) (a) Temporal and (b) spectral profiles at the output of 1.2-cm-long SOI waveguide when a 50 fs pulse propagates as a third-order soliton. The dotted curves show, for comparison, the corresponding input profiles.

In our numerical simulations, we propagate the 50-fs-wide third-order soliton inside a 1.2-cm-long SOI waveguide. Figure 2 shows the temporal and spectral profiles at the waveguide output. The features seen here can be understood in terms of soliton fission and Cherenkov radiation. The single third-order soliton evolves into three individual fundamental solitons in the time domain, as seen in Fig. 2(a). In Fig. 2(b), we see a spectral peak located at 1.31 μm. We have verified that this spectral feature corresponds to a dispersive wave that produces the long tail in Fig. 2(a). A similar feature occurs for silica fibers and is known to stem from the so-called Cherenkov radiation, emitted in the form of a dispersive wave at a frequency determined by the underlying phase-matching condition.[16] When solitons are mainly perturbed by the third-order dispersion β_3, the frequency of Cherenkov radiation is given by[16]

$$\Omega_d \approx -\frac{3\beta_2}{\beta_3} + \frac{\gamma P_s \beta_3}{3\beta_2^2}, \tag{6}$$

where P_s is the peak power of the fundamental soliton perturbed by β_3. In the absence of losses, $P_s = (5/3)^2 P_0$, where P_0 is the input peak power[2]; linear losses and TPA reduce this value all along the waveguide length. As a rough estimate, we use $P_s \approx P_0$ with $\beta_2 = -0.1701$ ps^2/m and $\beta_3 = 4.12 \times 10^{-3}$ ps^3/m in Eq. (6) and find that the wavelength of Cherenkov radiation is around 1.32 μm. This value agrees with numerical simulations shown in Fig. 2. The dominant spectral peak in this figure is redshifted by about 75 nm from the input wavelength. We have verified by setting $f_R = 0$ that this shift is mostly due to self-phase modulation and not due to SRS. In contrast with silica fibers, SRS plays a minor role in silicon because of its much narrower Raman-gain spectrum, and also the power-clamping effect of TPA.

Although the spectrum of the output pulse in Fig. 2 extends over 300 nm or so, it is not uniform enough to be useful for practical applications. We have studied the evolution of femtosecond pulses along the waveguide length under a variety of launch conditions. Our results indicate that soliton fission for $N = 3$ occurs within 3 mm after the pulse is launched, and a supercontinuum is formed soon after. In fact, the supercontinuum is much more uniform when it is first formed because it is not much affected by the TPA. As an example, Fig. 3 shows the output spectrum on a semilog scale at a distance of 3 mm under the conditions of Fig. 2. The 20 dB bandwidth is close to 420 nm in this case, which covers the entire telecommunication range from 1.3 to 1.7 μm.

To see what role TPA and FCA play over the 3 mm length, we have repeated the simulation with $\beta_{\mathrm{TPA}} = 0$ so that both of them are absent. The result is also shown in Fig. 3. Clearly, TPA reduces the bandwidth of supercontinuum but does not affect much of its flatness. The free carriers generated during this process have a negligible impact on the pulse because by the time enough free carriers accumulate at a certain location the 50 fs pulse moves away from that spot.

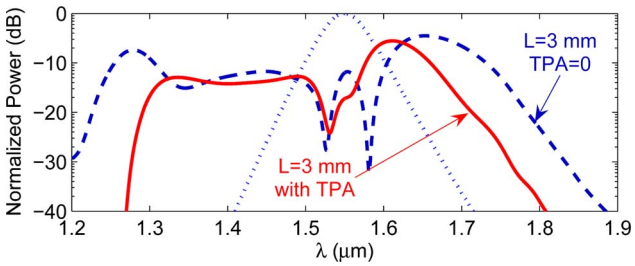

Fig. 3. (Color online) Supercontinuum created in a 3-mm-long SOI waveguide under the conditions of Fig. 2. The dashed curve shows the spectrum when the effects of TPA and FCA are ignored. The dotted curve shows the input pulse spectrum.

We thus conclude that neither SRS nor FCA plays a significant role during supercontinuum formation in silicon waveguides.

In conclusion, SOI waveguides can be used to create a supercontinuum extending over 400 nm by launching femtosecond pulses and propagating them as higher-order solitons. The physical process behind supercontinuum formation is related to soliton fission, self-phase modulation, and generation of Cherenkov radiation. As low-energy ($\approx$1 pJ) pulses and relatively short waveguides ($<$1 cm) are sufficient for supercontinuum generation, the proposed scheme should prove useful in practical applications.

This work was supported by National Science foundation (grant ECS-0320816). We acknowledge helpful discussions with Da Zhang, F. Yaman, and N. Usechak.

References

1. J. K. Ranka and R. S. Windeler, Opt. Lett. **25**, 25 (2000).
2. G. P. Agrawal, *Nonlinear Fiber Optics*, 4th ed. (Academic, 2006).
3. R. Claps, D. Dimitropoulos, V. Raghumathan, Y. Han, and B. Jalali, Opt. Express **11**, 1731 (2003).
4. R. Claps, V. Raghunathan, D. Dimitropoulos, and B. Jalali, Opt. Express **12**, 2774 (2004).
5. G. W. Rieger, K. S. Virk, and J. Young, Appl. Phys. Lett. **84**, 900 (2004).
6. O. Boyraz, P. Koonath, V. Raghunathan, and B. Jalali, Opt. Express **12**, 4094 (2004).
7. H. Rong, Y. Kuo, A. Liu, M. Paniccia, and O. Cohen, Opt. Express **14**, 1182 (2006).
8. Q. Lin, J. Zhang, P. M. Fauchet, and G. P. Agrawal, Opt. Express **14**, 4786 (2006).
9. M. A. Foster, A. C. Turner, J. E. Sharping, B. S. Schmidt, M. Lipson, and A. L. Gaeta, Nature **441**, 960 (2006).
10. E. Dulkeith, Y. A. Vlasov, X. Chen, N. C. Panoiu, and R. M. Osgood, Opt. Express **14**, 5524 (2006).
11. L. Yin, Q. Lin, and G. P. Agrawal, Opt. Lett. **31**, 1295 (2006).
12. H. H. Li, J. Phys. Chem. Ref. Data **9**, 561 (1980).
13. T. E. Murphy, software available at http://www.photonics.umd.edu.
14. Q. Xu and M. Lipson, Opt. Lett. **31**, 341 (2006).
15. A. Zwick and R. Carles, Phys. Rev. B **48**, 6024 (1993).
16. N. Akhmediev and M. Karlsson, Phys. Rev. A **51**, 2602 (1995).